Materials Research. 2014; 17(3): 700-707
DOI: http://dx.doi.org/10.1590/S1516-14392014005000046

Synthesis and Characterization of Novel ZrO_2-SiO_2 Mixed Oxides

Milena Araújo Ferreira e Santos, Ivon Pinheiro Lôbo, Rosenira Serpa da Cruz*

Departamento de Ciências Exatas e Tecnológicas, Universidade Estadual de Santa Cruz – UESC, Rod. Jorge Amado, Km 16, CEP 45662-900, Ilhéus, BA, Brasil

Received: September 2, 2013; Revised: February 6, 2014

In this study the mixed oxides ZrO_2-SiO_2, were synthesized by the sol-gel method with a molar ratio of 95:5 (Si/metal) and characterized by X-ray diffraction, absorption-desorption of N_2, Fourier transform infrared spectroscopy, thermal gravimetric analysis, temperature-programmed desorption of ammonia, and acidity test by titration. The synthesized materials, which are amorphous to X-rays, are composed of a mixture of micro- and mesopores. They show a higher acid strength than the separate oxides, indicating that the ZrO_2 is highly dispersed in the silica matrix.

Keywords: *mixed oxides, heterogeneous catalyst, methylation, sulfation*

1. Introduction

The continuous evolution of science and the general call for the protection of the environment have created an increased demand for new technologies and new materials. This becomes evident by the progress in the improvement of high performance metallic and polymeric materials, semiconductors, ceramics, nanotechnology, and catalysts[1,2]. In particular, those materials which exhibit catalytic activity have attracted attention due to their broad and growing applicability in many industrial processes[3], from the petrochemical industry to the food sector[4-7].

Numerous studies can be found in the literature[8-13] regarding the development of new materials with catalytic properties. Among the various solids with industrial applications, the mixed oxides are capable of combining the chemical and mechanical properties of their constituting oxides[5]. Once formed, the mixed oxides display acidic sites due to the excess negative or positive charge or due to defects in the lattice[14,15]. Owing to these properties, the acidic mixed oxides play an important role in applications such as the cyclization of citronellal to isopulegol[16,17], isomerization of α-pinene and dehydration of 4-methyl-2-pentanol[18], Fischer-Tropsch process[19], ammonia oxidation[20], hydrogenation of alkenes[21], synthesis of alcohols[22], and biodiesel production[23].

Among the most frequently employed methods for the synthesis of mixed oxides are the coprecipitation[24], hydrothermal routes[25], sonochemical processes[26], the oxalate route[27], and the sol-gel process[28]. From all these processes, the sol-gel process (SGP) has attracted attention due to its versatility in the development of new materials, owing to the simplicity and flexibility of the synthesis, which permits the preparation of highly pure and homogeneous products with controlled porosity[29]. Moreover, this process is environmentally friendly compared to the traditional routes for the preparation of ceramics and glasses[30].

An important application for mixed oxides is the catalysis of the esterification reaction of the free fatty acids contained in oils and/or fats, as a preceding step in biodiesel production. At commercial scale, biodiesel is mainly produced with homogeneous alkaline catalysts, although this technology poses some disadvantages, for example, its requirement of high-quality feedstock with low content of free fatty acids and water, the difficulty of recovery and reutilization of the catalyst, and the generation of effluents, all of which contribute to increased production costs. Therefore, research activities have turned towards the development of heterogeneous catalysts that can be separated easily from the reaction medium, allow for more flexibility concerning feedstocks with higher contents of free fatty acids and water, and can be reused several times, besides avoiding the generation of larger amounts of effluents.

In this context, silica-supported zirconium oxide has emerged as catalyst because of its thermal and chemical stability, its higher resistance to deactivation compared to the isolated oxides, and its higher acidity[27,31-33].

Based on the above considerations, the objective of this work was the synthesis and characterization of the mixed oxide ZrO_2-SiO_2 as well as the modification of its acid force and its hydrophilic character, followed by an preliminary assessment of the catalyst in the esterification of oleic acid with methanol, aiming at a future application in the production of biodiesel from high free fatty acid feedstocks.

2. Experimental

2.1. *Synthesis of the solids*

The ZrO_2-SiO_2 catalysts were prepared by the sol-gel method[34], with a 95:5 molar ratio of Si/Metal. Initially, a pre-hydrolysis was performed by agitating a solution containing tetraethoxysilane (TEOS)/H_2O/ethanol/HNO_3 at 80 °C, for 3 hours. Thereafter, appropriate amounts of a solution of the metal oxide precursor ($ZrOCl_2.8H_2O$) with ethanol were added, maintaining the agitation for two more

*e-mail: roserpa@uesc.br

hours, at room temperature. Then, H_2O and concentrated HNO_3 were added, and the resulting solution was kept at room temperature for another two hours. The gels were obtained by evaporation of the solvent and dried for 6 hours at 80 °C, macerated, washed for removal of the chlorides, dried at 100 °C for two hours, washed with ethanol in the soxhlet extractor, and calcined at 500 °C for three hours. This catalyst will be referred to as ZrO_2-SiO_2.

In order to obtain methylated material, the synthesis was carried out as described above, except that a proportion of 1:1 of methyltriethoxysilane $MeSi(OEt)_3$/TEOS was added in the pre hydrolytic step. This catalyst will be referred to as ZrO_2-SiO_2-Me.

In order to obtain sulfated material *in situ,* the synthesis proceeded as described for catalyst ZrO_2-SiO_2, but with the addition of an amount of 4.1 mL sulfuric acid at the hydrolytic and condensation steps, instead of the nitric acid. This catalyst will be referred to as ZrO_2-SiO_2-SO_4^{2-}-is.

2.2. *Characterizations*

The X-ray diffractional patterns with CuK_α radiation was obtained using a Siemens D5000 diffractometer. The range examined was $2\theta = 5$ to 80°, and the speed was 4°. s^{-1}. The adsorption-desorption isotherms of nitrogen were obtained at -196 °C with a Micromeritics ASAP 2010. The sample was previously treated for 17 hours at 250 °C under nitrogen flow. The pore diameters, as well as the pore size distribution, were calculated by using the BJH (Barrett, Joyner and Halenda) for microporous solids, based on the nitrogen adsorption isotherm. The specific area was calculated with the BET (Brunauer, Emmett and Teller) equation in the region with low pressure (p/po = 0.200), and the micropore area and micropore volume were determined using the software t-*plot*.

Infrared spectra have been registered in the range 4000-400 cm^{-1} using Shimadzu spectrometer, with a resolution of 4 cm^{-1}. The samples were prepared as KBr pastilles, with a proportion of 1% of the solids. The TG-DTA analyses were conducted with a Shimadzu DTG - 60/60H. The samples of the solids were heated under nitrogen flow, from room temperatures up to 700-900 °C, at a rate of 40 °C min^{-1}, using aluminium oxide cells.

The profiles of the thermal programmed desorption of ammonia (TPD-NH_3) were obtained with a Micromeritics Chemsorb 2720. The samples were pre-treated for one hour at 300 °C, under helium flow of 25 mL.min^{-1} followed by cooling to room temperature in order to remove any physisorbed species on the surface of the sample. After this pre-treatment, the samples were submitted to a chemisorption step using ammonia in helium (9.9%, mol/mol) flow of 25 mL.min^{-1} at room temperature, for 30 minutes. Thereafter, the system was purged with helium at room temperature for 30 minutes. In order to remove the physisorbed ammonia molecules, the material was treated for 30 minutes at 150 °C under helium flow (25 mL.min^{-1}) and then cooled to room temperature. This step was followed by the thermal programmed desorption analysis, in which the sample was heated from room temperature to 1000 °C, at a rate of 10 °C min^{-1} and under helium flow (25 mL.min^{-1}). The amount of desorbed ammonia was monitored with a thermal conductivity detector. The acidity of the catalyst was determined from the quantification of Brønsted acid sites by titration[35]. Finally, 100 mg of the material was brought into contact with 20 mL of 0.1 mol L^{-1} NaOH for three hours with light agitation. Then, samples of the basic solution were separated and titrated with 0.1 mol L^{-1} HCl in order to verify the amount of NaOH which reacted with the material. Acidity was determined in mmol H^+ per gram of material.

The synthesized materials were assessed in an esterification reaction using oleic acid (model molecule) with methanol, in a Parr reactor with a working volume of 300 mL, using the following reaction conditions: the molar ratio of acid/alcohol was 6:1, the amount of catalyst corresponded to 3% of the mass of the oleic acid, and the temperature was 120 °C, for 3 hours. Preceding the reaction, the catalyst had been dried at 110 °C, for 3 hours.

3. Results and Discussion

3.1. *Synthesis of the solids*

The solids were synthesized by means of the sol-gel process (SGP), a comparatively simple method for the synthesis of mixed oxides, which promotes high homogeneity of the metal on the surface of the matrix, better control of particle size, and higher purity[36].

The TEOS was chosen as precursor for presenting low hydrolysis rates, which promotes high homogeneity for mixed oxides[37]. The solvent was ethanol, which prevents the separation of the liquid-liquid phases during the initial stage of hydrolysis, and consequently, the concentrations of water and silicate are maintained, which influence the reaction speed in the gelation step. Furthermore, ethanol facilitates the drying process due to its high vapor pressure. The drying process by slow evaporation of the ethanol as well as the thermal treatment with low heating rates led to the formation of a xerogel[38,39].

The synthesis route was catalyzed by a nitric acid (HNO_3) with a (HNO_3:TEOS–$1{,}2x10^{-4}$) molar ratio, in order to produce a linear polymeric system with few ramifications. The acid hydrolysis started with a pre-hydrolysis of the lesser hydrolysable precursor to ascertain the adequate control of the number of hydrolyzed sites of the TEOS. This procedure favors the condensation in linear polymer chains and high homogeneity of the oxides, because the silicon alkoxides have lower reactivity than those of the metal transition precursors[39].

The evaporation of ethanol and water in environmental conditions during the hydrolization/condensation step for the synthesized materials promoted the increase of the mean diameter of the pores.

Modifying the surface of the catalyst by the substitution of 50% of the TEOS by $MeSi(OEt)_3$ during the SGP (part 2.1- represented by ZrO_2-SiO_2- Me) produced a material with lesser hydrophilic character due to the exchange of the acidic hydrogens of the silanol groups (Si-OH) by methyl groups (–CH_3), as shown in Figure 1. Therefore, this material is expected to be more resistant to deactivation by the water produced during the esterification reaction.

The sulfation of the ZrO_2-SiO_2 material was conducted with to increase the acid force for some relevant reactions.

The *in situ* sulfation of the material in the SGP process was studied, where the sulfuric acid was added in the sol-stage. Therefore, the formation of sulfate groups is expected which strongly bond to the lattice. This can be explained by the interaction of the aqueous complexes of Zr^{4+} with the sulfate ions, forming species of the type $[Zr(OH)_2(SO_4^{2-})_x\ (H_2O)_y]_n^{n(2-2x)}$, which can interact strongly with the silica in the solution and which exhibit a negative charge under the employed synthesis conditions. It can therefore be concluded that the method of sulfation *in situ* provided a better distribution of the sulfated zirconium between the surface and the lattice of the material[40,41].

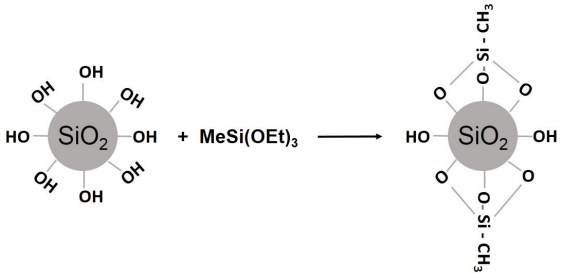

Figure 1. Diagram of the modification of the silicon surface.

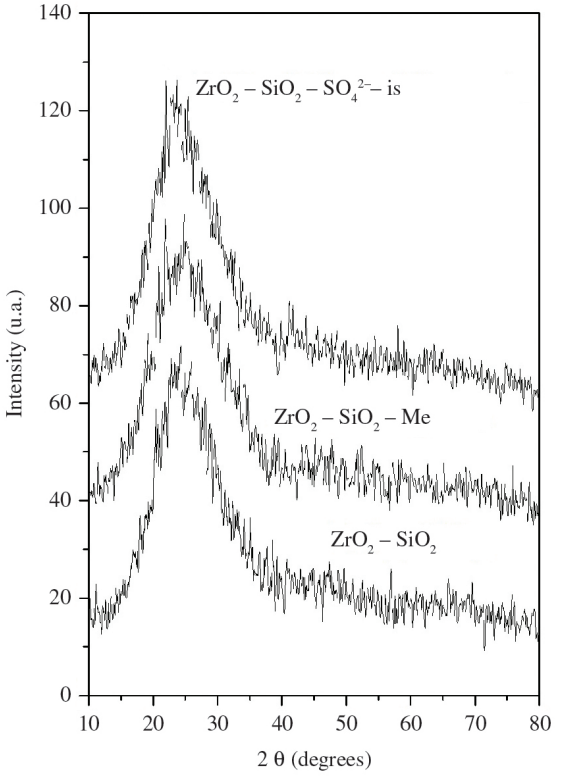

Figure 2. X-ray diffractional patterns of the samples ZrO_2-SiO_2, ZrO_2-SiO_2-Me, and ZrO_2-SiO_2- SO_4^{2-}-is.

3.2. *Characterization*

The characterization was done in order to verify if the different synthesis conditions promoted the formation of mixed oxides with high dispersion of the zirconium oxide in the silica matrix and narrow pore distribution.

The analysis of the X-ray diffractional patterns for all of the materials in Figure 2 shows only wide peaks varying between 15° and 30°, which are attributed to SiO_2 in its amorphous state. This indicates that the synthesis methods used promoted a high dispersion of the ZrO_2 in the amorphous silica matrix[31,32,42,43].

As discussed in section 3.1, and suggested by the results of the X-ray diffraction, the pre-hydrolysis of the TEOS promoted the production of highly homogeneous materials.

The evaluation of the textural characterization of the solids was based on the adsorption-desorption isotherms of N_2 at -196.15 °C and revealed different textures of the solids. Figures 3 and 4 show the isotherms of adsorption-desorption of N_2 and the distribution curves of the pore volumes for synthesized materials.

The materials showed type IV isotherms with a combination of hysteresis types (H2 and H3), which indicate the presence of micropores as well as mesopores. The total pore volume, the micropore area and the micropore volume, calculated with t-plot, confirmed these observations (Table 1).

The distribution curves of pore diameter shown in Figure 4 as well as the data in Table 1 show that all the synthesized materials have an even monomodal pore-size distribution with mean pore diameters ranging from 3.3 to 3.7 nm, which classifies them as mesoporous solids according to IUPAC[28,44].

Partial substitution of hydroxyl groups by methyl-CH_3 groups in the ZrO_2-SiO_2 material induces an increase in pore diameter (Table 1). This may be due the decrease of the interaction of the hydrogen bonds between the water and the OH-groups on the inner walls of the pores, promoting a reduction of the internal tension during the drying process[45]. The insertion of sulfate groups to the ZrO_2SiO_2-$SO_4^{2-}$is materials resulted in a decrease of the specific area and increase of the mean pore diameter (Table 1). The presence of sulfate ions in the micropores partially blocks the pores, makes them inaccessible to N_2 molecules, and consequently influences the size of the area. The increase in pore diameter can be linked to the presence of sulfate ions on the micropore walls, causing tension and rupture, followed by increased micropore volume and diameter[42].

The spectra in the infrared region shown in Figure 5 indicate the presence of a band at 1630 cm^{-1} that corresponds to scissor bending vibration of the H-O-H bond of the physisorbed molecular water[27,42,46,47].

The samples showed bands centered at 1078 cm^{-1} with a shoulder at ~ 1220 cm^{-1} due to the asymmetric Si-O-Si stretching vibrations of transverse-optical (TO_3) mode and the longitudinal-optic (LO_3) part stretching vibrations, respectively[47]. Bands observed around 800 cm^{-1} and 460 cm^{-1} are due to TO symmetric stretching and bending vibrations of Si-O-Si bonds, respectively[47,48].

Bands with frequency mode from 910 cm^{-1} to 975 cm^{-1} can be assigned to Si-O- groups in SiO_2 gel or to stretching

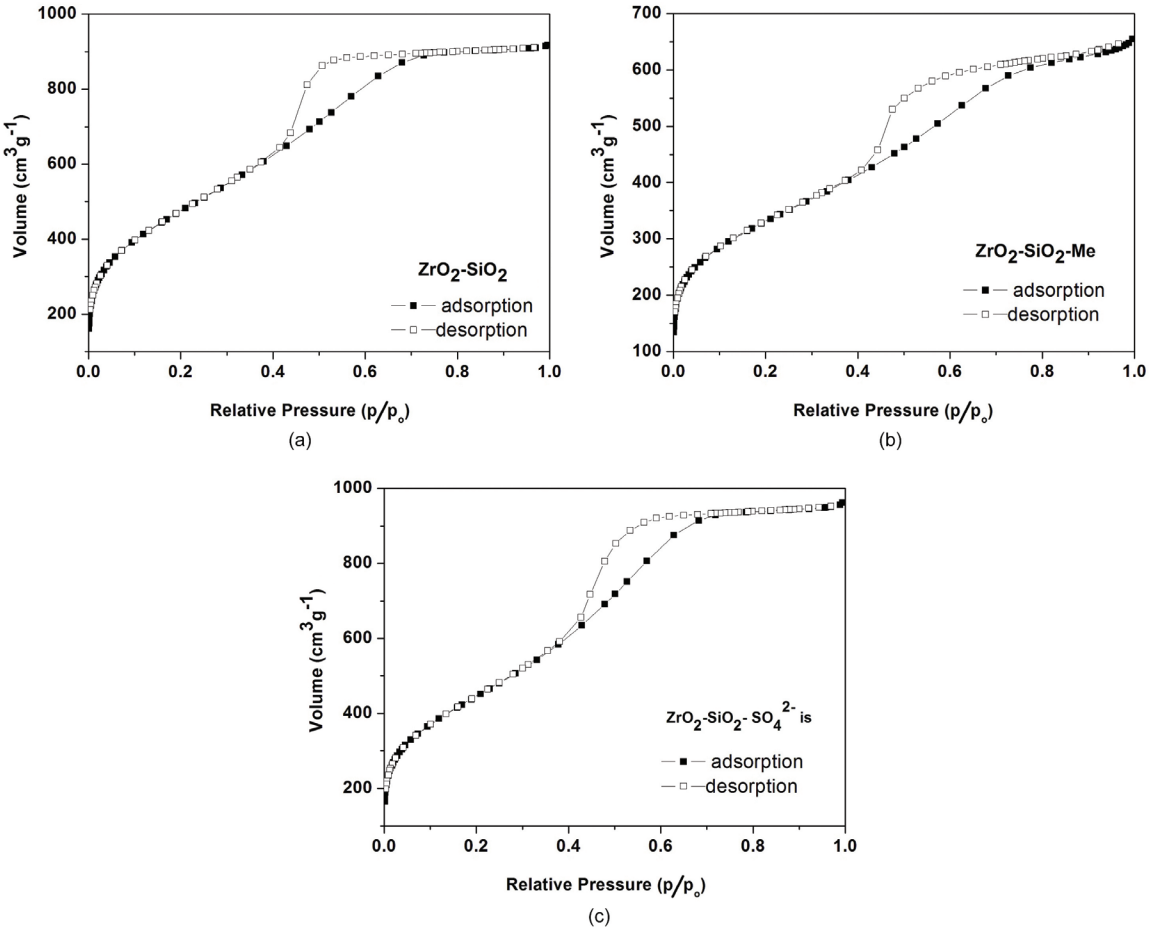

Figure 3. N_2 adsorption-desorption isotherms for the catalysts: (a) ZrO_2-SiO_2,)(b) ZrO_2-SiO_2-Me, and (c) ZrO_2-SiO_2- SO_4^{2-}-is.

Table 1. Specific area, micropore area, mean pore diameter, volume of micropore and total pore volume of the synthesized materials.

Material	Specific area BET (m^2g^{-1})	Micropore area (m^2g^{-1})	Specific area BET (m^2g^{-1})	Mean pore diameter BJH (nm)	Micropore volume t-plot (cm^3g^{-1})	Total pore volume (cm^3g^{-1})
ZrO_2-SiO_2	1742	1079	1742	3.3	0.77	1.40
ZrO_2-SiO_2-Me	1181	610	1181	3.7	0.39	0.96
ZrO_2SiO_2-SO_4^{2-}-is	1639	992	1639	3.5	0.84	1.46

vibration modes of the Si-O-Zr groups in ZrO_2-SiO_2 binary oxides[31,40,46]. Typically, bands placed at higher frequencies are assigned to Si-O-Zr groups[47]. These features confirm the results of the DRX, suggesting the production of X-ray amorphous or poor crystalline materials and incorporation of ZrO_2 into silicate matrix.

The analysis of the thermogravimetric curves of the materials in Figure 6 shows the almost constant decrease of mass in the range of 100 to 200 °C, which is due to the elimination of water, impurities, alkoxides, and unreacted solvents. Above 700 °C, the loss of mass is associated with the dehydroxilation of the surface[27].

The usually characteristic band of Si-C at 1276 cm^{-1} for the ZrO_2-SiO_2-Me catalyst in the FTIR analysis (Figure 5) could not be verified due to the small amount of $MeSi(OEt)_3$ used for synthesis. The thermal analysis (Figure 6b) revealed the existence of a wide peak reaching from 596 to 793 °C, which is considered to result from alcoxides that have not reacted, and from the breaking of the Si-C-bonds, an evidence for the insertion of the methyl group. Based on this information, the calcination temperature of these materials was determined, because at temperatures above 500 °C the methylated groups decompose, compromising the reaction[37]. Besides, it is noteworthy that the loss of water attributed to the methylated catalyst (ZrO_2-SiO_2-Me) is smaller when compared with other materials, and corresponds with the lesser hydrophilic character expected for this sample.

The thermal programmed ammonia desorption (TPD-NH_3) shown in Figure 7 for the ZrO_2-SiO_2 and ZrO_2-SiO_2-SO_4^{2-}-is catalysts reflects the strength and distribution of the acid sites at the desorption temperature of ammonia.

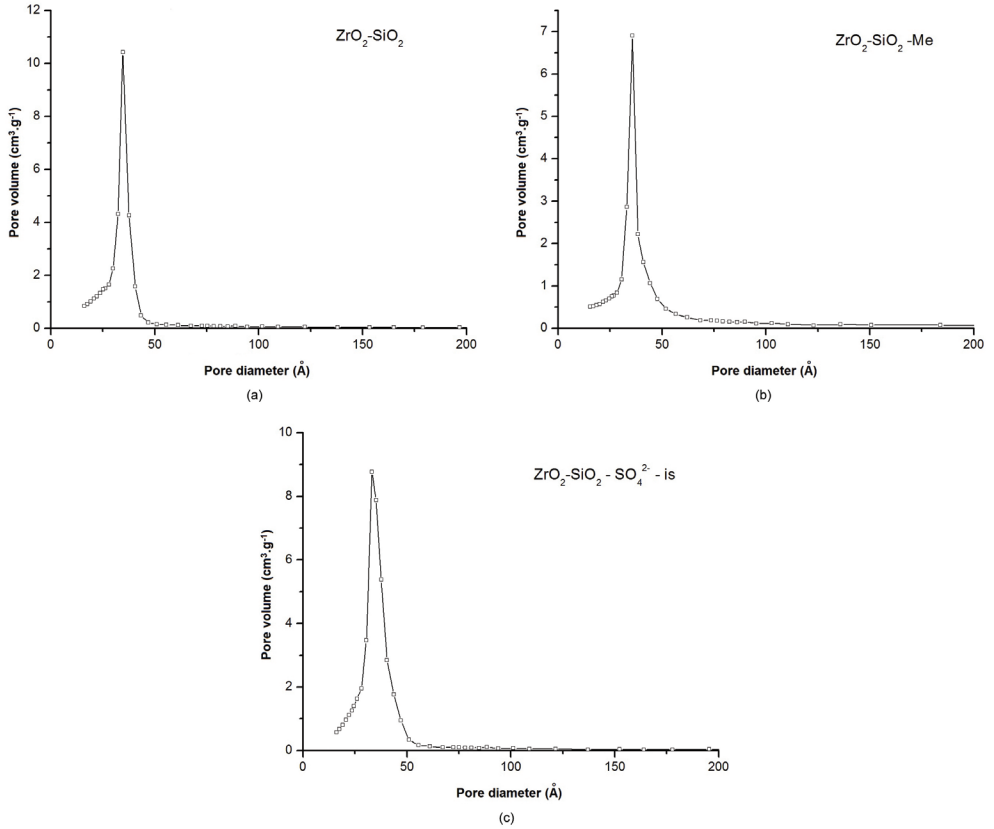

Figure 4. Distribution curves for the pore diameter of the catalysts: (a) ZrO_2-SiO_2, (b) ZrO_2-SiO_2-Me, and (c) ZrO_2SiO_2-SO_4^{2-}-is.

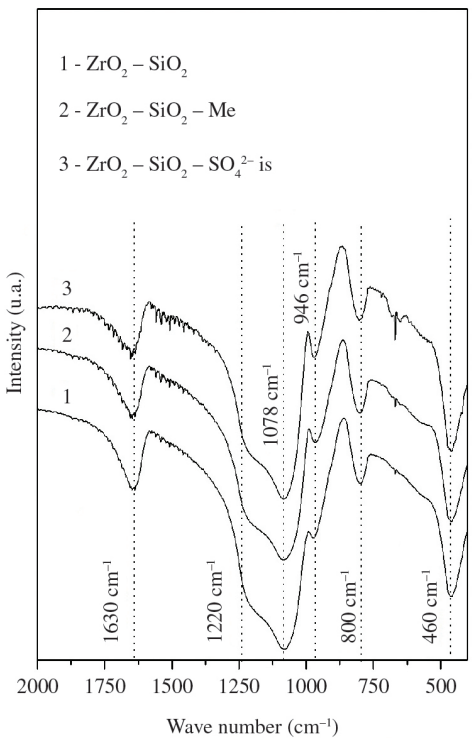

Figure 5. Spectra in the infrared region for the samples: 1) ZrO_2-SiO_2, 2) ZrO_2-SiO_2-Me, 3) ZrO_2-SiO_2- $SO_4^{2-}$is.

Table 2. Acidity by titration of materials.

Catalysts	Concentration of H^+ (mmol/g)
ZrO_2-SiO_2	476
ZrO_2-SiO_2-Me	184
ZrO_2-SiO_2-SO_4^{2-}-is	380

The materials without sulfation (Figure 7a) showed three defined peaks at 132, 328, and 506 °C that are related to weak, intermediate and strong acid sites, respectively. The occurrence of these sites can be attributed to the defects on the surface due to the insertion of zirconia in the silica matrix and the formation of bonds of the Si-O-Zr-O-Zr as well as the, Zr-O e Zr=O bands[49].

The presence of the desorption peaks at 310 °C with a shoulder at 182 °C and 618 °C (Figure 7b) suggest, respectively, the existence of weak/intermediate and strong/superacid sites in the sulfated material.

The increase of acidity in the sulfated material was observed based on the analysis of TPD-NH_3 (Figure 7) and confirmed by the acidity test by titration of NaOH (Table 2), and revealed the presence of acid/superacid sites for the sulfated materials.

The acidity of the materials produced by the titration with NaOH, which only identifies Brønsted acid sites, is consistent with the results of the TDP-NH_3 (Figure 7), where the sulfation favored the formation of Lewis acid sites and

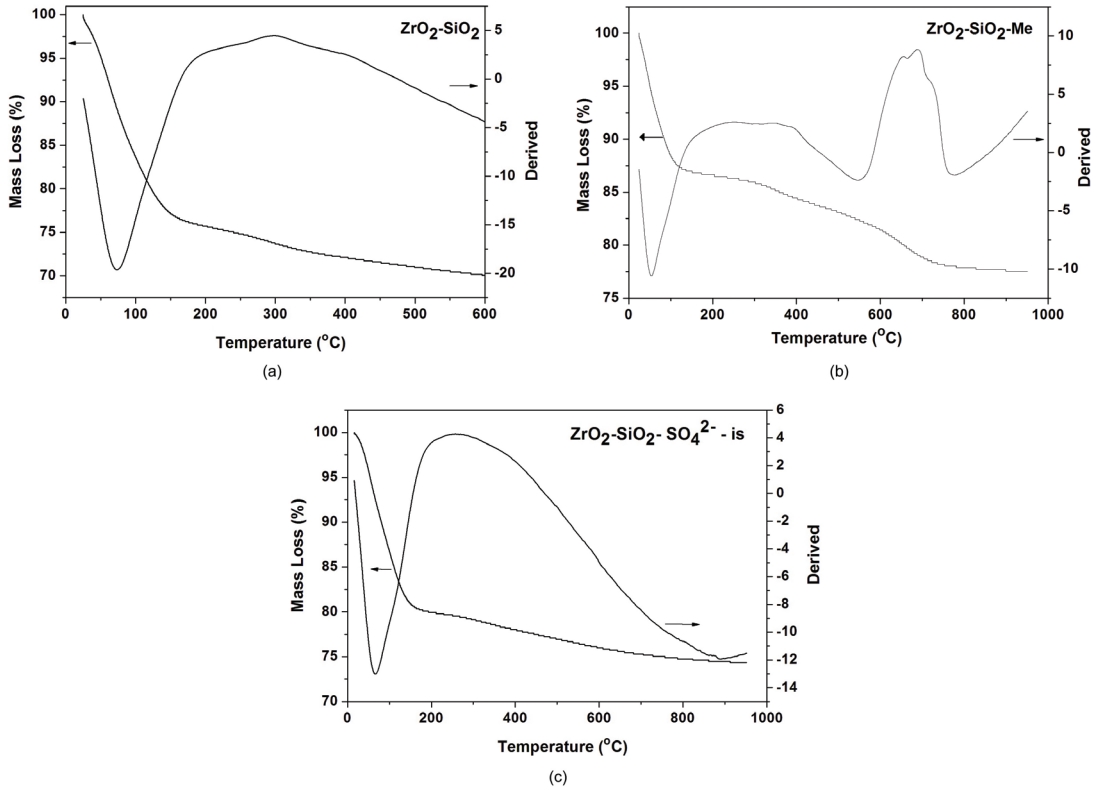

Figure 6. TGA of samples: (a) ZrO_2-SiO_2 (b) ZrO_2-SiO_2-Me and (c) ZrO_2-SiO_2-SO_4^{2-}-is.

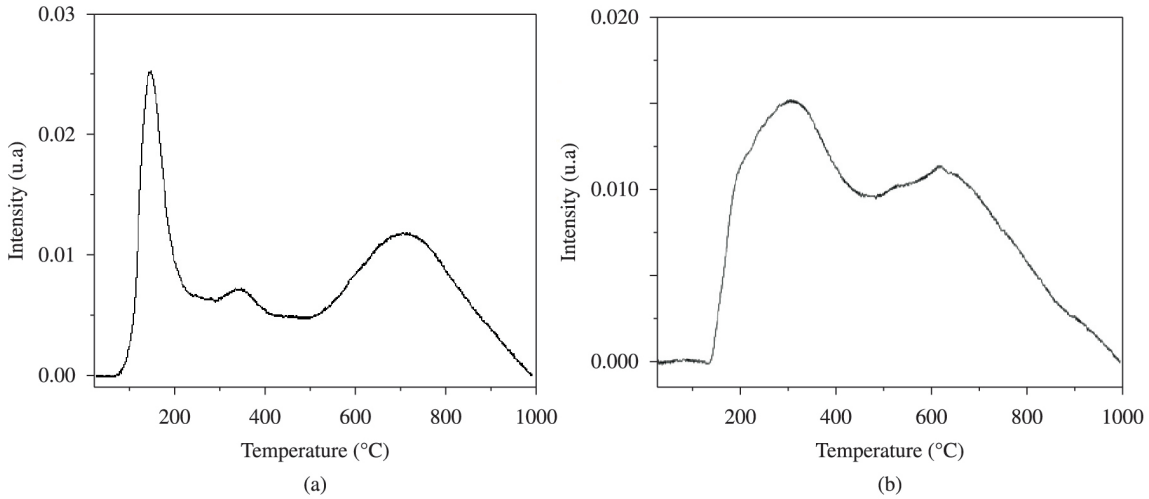

Figure 7. Graph of the thermal programmed desorption curve of ammonia for the catalysts a) ZrO_2-SiO_2; b) ZrO_2-SiO_2-SO_4^{2-}-is.

led to a decrease of Brønsted acid sites as shown in Table 2. As the Lewis acid sites are stronger than the Brønsted acid sites, the *in situ* sulfated mixed oxide shows a higher concentration of strong acid sites than the standard material (ZrO_2-SiO_2). It is suggested that the increase in Lewis acid sites after sulfation is associated with the formation of Zr-SO_4[49]. After the methylation of the mixed oxide ZrO_2-SiO_2, a distinct decrease of Brønstedt acidity was observed, which is probably due to the substitution of silanol groups by methyl groups at the surface.

The solids ZrO_2-SiO_2, ZrO_2-SiO_2-Me e ZrO_2-SiO_2-SO_4^{2-}-is were tested for their catalytic activity in an esterification reaction of oleic acid with methanol, which resulted in ester conversions of 40.8, 49.8 and 49.4%, respectively. As expected, the modified materials ZrO_2-SiO_2-Me and ZrO_2-SiO_2-SO_4^{2-}-is showed the best catalytic activity. The catalyst ZrO_2-SiO_2-Me displays a hydrophobic surface which minimizes blocking of active sites of the material, This is due to the anchoring of water molecules from the esterification reaction[46,50]. For the catalyst ZrO_2-SiO_2-

SO_4^{2-} - is, the conversion percentage in the esterification reaction is due to the acidity caused by the incorporation of sulfate into its structure.

The materials were promising in relation to their catalytic activity in the esterification reaction. In a next step, these solids will be evaluated with regard to their stability to leaching of the active species to the reaction medium and to the possibility of their reuse in the reaction. Following this, the reaction conditions will be optimized to improve ester yields.

4. Conclusions

X-ray amorphous, meso- to microporous mixed oxides were produced by the sol-gel method, with highly dispersed zirconium on the silica matrix, as verified by the techniques DRX e FTIR. In the mixed oxide ZrO_2SiO_2 – Me, the surface polarity was modified through the substitution of silanol groups by methyl groups, as evidenced by the TGA/DTA technique. The mixed oxide ZrO_2-SiO_2-SO_4^{2-} - is showed a higher distribution of acidic sites after sulfatation *in situ*, as confirmed by the TPD-NH_3 technique.

The preliminary tests of the catalytic activity showed that the modifications of the mixed oxide ZrO_2SiO_2 contributed considerably to the increase of the conversion of the esterification reaction of oleic acid with methanol. The synthesized materials can therefore be considered promising catalysts for esterification reactions in the context of biodiesel production.

Acknowledgments

We gratefully acknowledge funding provided by the Fundação de Apoio à Pesquisa do Estado da Bahia (FAPESB) and the Conselho Nacional de Desenvolvimento Científico e Tecnológico (CNPq). MAFS would like to acknowledge Coordenação de Aperfeiçoamento de Pessoal de Nível Superior (CAPES) for a Master's scholarship.

References

1. Callister WD Jr. *Ciência e engenharia de materiais: uma introdução.* Rio de Janeiro: LTC Editora Ltda; 2008. p. 2-10.
2. Shackelford JF. *Introdução à ciência dos materiais para engenheiros.* São Paulo: Pearson Prentice Hall Editora; 2008. p. 2-12.
3. Armor JN. A history of industrial catalysis. *Catalysis Today*. 2011; 163:03-09. http://dx.doi.org/10.1016/j.cattod.2009.11.019
4. Schmal M. *Catálise Heterogênea*. Rio de Janeiro: Synergia Editora; 2011. p. 2-7.
5. Sanchez C, Belleville P, Popall M and Nicole L. Applications of advanced hybrid organic–inorganic nanomaterials: from laboratory to market. *Chemical Society Review*. 2011; 40:696-753. http://dx.doi.org/10.1039/c0cs00136h
6. Santos EN and Lago RM. Publicações na área de catálise envolvendo instituições brasileiras: uma comparação entre os periódicos especializados e os da SBQ. *Quimica Nova*. 2007; 30(6):1480-1483. http://dx.doi.org/10.1590/S0100-40422007000600017
7. Ciola R. *Fundamentos da Catálise*. São Paulo: Moderna Editora; 1981. p. 1-16.
8. Gonçalves G, Lenzi MK, Santos OAA and Jorge LMM. Preparation and characterization of nickel based catalysts on silica, alumina and titania obtained by sol–gel method. *Journal of Non-Crystalline Solids*. 2006; 352:3697-3704. http://dx.doi.org/10.1016/j.jnoncrysol.2006.02.120
9. Giordano C and Antonietti M. Synthesis of crystalline metal nitride and metal carbide nanostructures by sol–gel chemistry. *Nano Today*. 2011; 6:366-380. http://dx.doi.org/10.1016/j.nantod.2011.06.002
10. Gross S and Muller K. Sol–gel derived silica-based organic–inorganic hybrid materials as "composite precursors" for the synthesis of highly homogeneous nanostructured mixed oxides: an overview. *Journal Sol-Gel Science Technology*. 2011; 60:283-298. http://dx.doi.org/10.1007/s10971-011-2565-x
11. Segota S, Cúrkovic L, Ljubas D, Svetlicic V, Houra IF and Tomasic N. Synthesis, characterization and photocatalytic properties of sol–gel TiO_2 films. *Ceramics International*. 2011; 37:1153-1160. http://dx.doi.org/10.1016/j.ceramint.2010.10.034
12. Souza AJ, Pinheiro BCA and Holanda JNF. Influência da incorporação de resíduo de rocha ornamental sobre as propriedades e microestrutura sinterizada de piso cerâmico. *Revista Matéria.* 2013; 18(1):19-28. http://dx.doi.org/10.1590/S1517-70762013000100004
13. Garrido FMS, Medeiros RF, Nogueira NOB, Peres RCD, Ribeiro ES and Medeiros ME. Síntese de óxidos mistos SiO_2/Mn_xO_y para aplicação na reação de redução de O_2. *Revista Matéria.* 2013; 18(2):1294-1305. http://dx.doi.org/10.1590/S1517-70762013000200005
14. Tanabe K and Yamaguchib T. Acid-base bifunctional catalysis by ZrO_2 and its mixed oxides. *CatalysisToday*. 1994; 20:185-198. http://dx.doi.org/10.1016/0920-5861(94)80002-2
15. Soled S and McVicker GB. Acidity of silica-substituted zirconia. *Catalysis Today*. 1992; 14:189-194. http://dx.doi.org/10.1016/0920-5861(92)80022-F
16. Ravasio N, Antenori M, Barburdri F and Gargano M. Intramolecular Ene reactions promoted by mixed cogels. *Studies in Surface Science Catalysis.* 1997; 108:625-632. http://dx.doi.org/10.1016/S0167-2991(97)80959-7
17. Jimeno C, Miras J and Esquena J. $TiO_2(SiO_2)_x$ and $ZrO_2(SiO_2)_x$ Cryogels as Catalysts for the Citronellal Cyclization to Isopulegol. *Catalysis Letter*. 2013; 143:616-623. http://dx.doi.org/10.1007/s10562-013-1007-5
18. Sidhpuria KB, Tyagi B and Jarsa RV. ZrO_2–SiO_2 Mixed Oxides Xerogel and Aerogel as Solid Acid Catalysts for Solvent Free Isomerization of α-Pinene and Dehydration of 4-Methyl-2-Pentanol. *Catalysis Letter*. 2011; 141:1164. http://dx.doi.org/10.1007/s10562-011-0602-6
19. Ko C-H, Yeh K-W, Wang Y-N, Wu C-H, Chang F-C, Cheng M-H et al. Impact of methanol addition strategy on enzymatic transesterification of jatropha oil for biodiesel processing. *Energy*. 2012; 48:375-379. http://dx.doi.org/10.1016/j.energy.2012.06.042
20. Wang Z, Qu Z, Quan X and Wang H. Selective catalytic oxidation of ammonia to nitrogen over ceria–zirconia mixed oxides. *Applied Catalysis A: General*. 2012; 114:131-138. http://dx.doi.org/10.1016/j.apcata.2011.10.030
21. Boudjahem AG, Bouderbala W and Bettahar M. Benzene hydrogenation over Ni–Cu/SiO_2 catalysts prepared by aqueous hydrazine reduction. *Fuel Processing Technology*. 2011; 92:500-506. http://dx.doi.org/10.1016/j.fuproc.2010.11.003

22. Kantam ML, Reddy RS, Pal U, Sudhakar M, Venugopal A, Ratnam KJ et al. Ruthenium/magnesium–lanthanum mixed oxide: An efficient reusable catalyst for oxidation of alcohols by using molecular oxygen. *Journal of Molecular Catalysis A: Chemical*. 2012; 359:1-7. http://dx.doi.org/10.1016/j.molcata.2012.03.013
23. Farooq M, Ramli A and Subbarao D. Biodiesel production from waste cooking oil using bifunctional heterogeneous solid catalysts. *Journal of Cleaner Production*. 2013; 59:131-140. http://dx.doi.org/10.1016/j.jclepro.2013.06.015
24. Mei Y, Cui M, Zhang N, Long Z and Huang X. Characterization of CeO_2-ZrO_2 mixed oxides prepared by two different co-precipitation methods. *Journal of Rare Earths*. 2013; 31(3):251-256. http://dx.doi.org/10.1016/S1002-0721(12)60267-1
25. Piticescu R, Monty C and Millers D. Hydrothermal synthesis of nanostructured zirconia materials: Present state and future prospects. *Sensors and Actuators B*. 2005; 109:102-106. http://dx.doi.org/10.1016/j.snb.2005.03.092
26. Liang J, Jiang X, Liu G, Deng Z, Zhuang J, Li F et al. Characterization and synthesis of pure ZrO_2 nanopowders via sonochemical method. *Material. Research. Bulletin*. 2003; 38:161-168. http://dx.doi.org/10.1016/S0025-5408(02)01007-3
27. Chandradass J, Han KS and Bae DS. Synthesis and characterization of zirconia- and silica-doped zirconia nanopowders by oxalate processing.Journal *of Materials Processing Technology*. 2008; 206:315-321. http://dx.doi.org/10.1016/j.jmatprotec.2007.12.034
28. Avendano RRG, Reyes De Los JA, Viveros T and Montoya De La Fuente JA. Synthesis and characterization of mesoporous materials: Silica–zirconia and silica–titania. *Catalysis Today*. 2009; 148:12-18. http://dx.doi.org/10.1016/j.cattod.2009.07.097
29. Avnir D, Coradin T, Lev O and Livage J. Recent bio-applications of sol–gel materials. *Journal Material. Chemical*. 2006; 16:1013-1030. http://dx.doi.org/10.1039/b512706h
30. Baccile N, Babonneau F, Thomas B and Coradin T. Introducing ecodesign in silica sol–gel materials. *Journal of Materials Chemistry.* 2009; 19:8537-8559. http://dx.doi.org/10.1039/b911123a
31. Zhang Y, Pan L, Gao C and Zhao Y. Synthesis of ZrO_2–SiO_2 mixed oxide by alcohol-aqueous heating method. *Journal Sol-Gel Science Technology.* 2011; 58:572-579. http://dx.doi.org/10.1007/s10971-011-2429-4
32. Zhang Y, Pan L, Gao C, Wang Y and Zhao Y. Preparation of ZrO_2–SiO_2 mixed oxide by combination of sol–gel and alcohol-aqueous heating method and its application in tetrahydrofuran polymerization. *Journal Sol-Gel Science Technology.* 2010; 56:27-32. http://dx.doi.org/10.1007/s10971-010-2268-8
33. Zhan Z and Zeng HC. A catalyst-free approach for sol–gel synthesis of highly mixed ZrO_2–SiO_2 oxides. *Journal of Non-Crystalline Solids*. 1999; 243:26-38. http://dx.doi.org/10.1016/S0022-3093(98)00810-2
34. Cardoso WS, Francisco MSP, Lucho AMS and Gushikem Y. Synthesis and acidic properties of the SiO_2/SnO_2 mixed oxides obtained by the sol–gel process. Evaluation of immobilized copper hexacyanoferrate as an electrochemical probe. *Solid State Ionics.* 2004; 167:165-173. http://dx.doi.org/10.1016/j.ssi.2003.12.017
35. Brum SS, Santos VC, Destro P and Guerreiro MC. Esterificação de ácidos graxos utilizando zircônia sulfatada e compósitos carvão ativado/zircônia sulfatada como catalisadores. *Química Nova*. 2011; 34(9):1511-1516. http://dx.doi.org/10.1590/S0100-40422011000900006
36. Hargreaves JSJ and Jackson D. *Metal oxide catalysis*. Weinheim: Editora Wiley-VDH Verlag Gmbh; 2009.
37. Cruz RS. *Óxidos mistos e microporosos preparados pelo método sol-gel como catalisadores para a oxidação de hidrocarbonetos em fase líquida.* [Tese]. Campinas: Universidade Estadual de Campinas; 2001.
38. Cardoso WS. *Óxidos mistos de SiO_2/SnO_2, SiO_2/SnO_2/ Fosfatos: propriedades e aplicações.* [Tese]. Campinas: Universidade Estadual de Campinas; 2005.
39. Canevari TC. *Ftalocianina de cobalto preparado in situ sobre o óxido misto SnO_2/SiO_2 obtidos pelo processo sol-gel. Aplicação na oxidação eletrocatalítica do ácido oxálico e do nitrito.* [Dissertação]. Campinas: Universidade Estadual de Campinas; 2008.
40. Chen XR, Ju YH and Mou CY. Direct Synthesis of Mesoporous Sulfated Silica-Zirconia Catalysts with High Catalytic Activity for Biodiesel via Esterification. *Journal Physical Chemical*. 2007; 111:18731-18737.
41. Ciesla U, Froba M, Stucky G and Schuth F. Highly Ordered Porous Zirconias from Surfactant-Controlled Syntheses: Zirconium Oxide–Sulfate and Zirconium Oxo Phosphate. *Chemistry Materials*. 1999; 11:227-234. http://dx.doi.org/10.1021/cm980205v
42. Tyagi B, Sidhpuria KB, Shaik B and Jasra RV. Effect of Zr/Si molar ratio and sulfation on structural and catalytic properties of ZrO_2–SiO_2 mixed oxides. *Journal Porous Materials*. 2010; 17:699-709. http://dx.doi.org/10.1007/s10934-009-9341-0
43. Avendano RRG and Reyes De Los JA. Effect of Synthesis Parameters on Sol–Gel Silica Modified by Zirconia. *Journal of Sol-Gel Science and Technology*. 2005; 33:133-138. http://dx.doi.org/10.1007/s10971-005-6714-y
44. Leofanti G, Padovan M, Tozzola G and Venturelli B. Surface area and pore texture of catalysts. *Catalysis Today*. 1998; 41:207-219. http://dx.doi.org/10.1016/S0920-5861(98)00050-9
45. Schmidt H. Chemistry of material preparation by the sol-gel process. *Crystalline Solids*. 1988; 100:51-64. http://dx.doi.org/10.1016/0022-3093(88)90006-3
46. Jiménez-Morales I, Río-Tejero Del MA, Braos-García P, Santamaría-González J, Maireles-Torres P and Jiménez-López A. Preparation of stable sulfated zirconia by thermal activation from a zirconium doped mesoporous MCM-41 silica: Application to the esterification of oleic acid with methanol. *Fuel Processing Technology*. 2012; 97:65-70. http://dx.doi.org/10.1016/j.fuproc.2012.01.014
47. Saha SK and Pramanik P. Aqueous sol-gel synthesis of powders in the ZrO_2–SiO_2 system using zirconium formate and tetraethoxysilane. *Journal of Non-Crystalline Solids*. 1993; 159:31-37. http://dx.doi.org/10.1016/0022-3093(93)91279-C
48. Monte F, Larsen W and MacKenzie JD. Chemical Interactions Promoting the ZrO_2 Tetragonal Stabilization in ZrO_2–SiO_2 Binary Oxides. *Journal American. Ceramic. Society*. 2000; 83(6):1506-12. http://dx.doi.org/10.1111/j.1151-2916.2000.tb01418.x
49. Li R, Yu F, Li F, Zhou M, Xu B and Xie K. One-pot synthesis of superacid catalytic material SO_4^{2-}/ZrO_2–SiO_2 with thermostable well-ordered mesoporous structure. *Journal of Solid State Chemistry*. 2009; 182:991-994. http://dx.doi.org/10.1016/j.jssc.2008.04.009
50. Lam MK, Lee KT and Mohamed AR. Homogeneous, heterogeneous and enzymatic catalysis for transesterification of high free fatty acid oil (waste cooking oil) to biodiesel: A review. *Biotechnology Advances*. 2010; 28:500-518. http://dx.doi.org/10.1016/j.biotechadv.2010.03.002